

## Axisymmetric Hollowing Instability of an Intense Relativistic Electron Beam Propagating in Air

C. A. Ekdahl, J. R. Freeman, G. T. Leifeste, R. B. Miller, and W. A. Stygar  
Sandia National Laboratories, Albuquerque, New Mexico 87185

and

B. B. Godfrey  
Mission Research Corporation, Albuquerque, New Mexico 87106  
(Received 22 March 1985)

Simulations of relativistic electron beams propagating in air show axisymmetric hollowing instabilities of the beam, caused by avalanche ionization of the air near the beam axis. This produces an induced return current peaked on axis, which weakens the pinch force there and triggers the instability for  $E/p > 130 \text{ kV cm}^{-1} \text{ atm}^{-1}$  and current neutralization  $> 50\%$ . We performed experiments verifying the existence of this instability on a 6-kA/ns, 70-kA, 4-MeV beam for air pressures less than  $\sim 80$  Torr, the predicted threshold.

PACS numbers: 41.80.Dd, 52.35.Py, 52.40.Mj, 52.65.+z

A relativistic electron beam in air is rapidly space-charge neutralized as a result of conductivity generated by beam-impact ionization and secondary-electron avalanche. The self-pinched beam<sup>1,2</sup> can propagate efficiently if the beam current is partially neutralized by the induced return current so that the net current is less than the Alfvén limit,  $I_A = \gamma\beta mc^3/e$ , where  $\gamma mc^2$  is the electron energy and  $\beta = v/c$ . There is, however, cause for concern about the stability of a propagating beam. Resistive instabilities result from diffusive phase lags of the magnetic fields in the weakly ionized gas.<sup>3-5</sup> In addition, the magnetic repulsion of the beam electrons by the return current induced in the ionized gas is a powerful destabilizing mechanism.<sup>6-10</sup> The instability can take the form of an axisymmetric hollowing with azimuthal mode number  $m = 0$ , and radial mode number  $n = 2$ . Hollowing can occur even if the beam is otherwise stable to the  $m = 1$  resistive-hose instability, which has long been considered the most dangerous mode on a beam propagating in gas. We report here the first experimental observations of the return-current-driven axisymmetric hollowing of a 4-MeV, 70-kA beam propagating in air.

Particle-in-cell numerical simulations indicate that the hollowing instability results from avalanche ionization near the beam axis.<sup>10</sup> As a consequence, the induced return current is concentrated near the axis, weakening the self-pinching force. If this return-current profile is generated early in the beam, then succeeding beam segments can lose their self-pinched equilibrium, and rapidly evolve to a hollow profile. The radius of these hollow segments increases rapidly in the region of instability, sometimes reaching a hollow equilibrium<sup>11-13</sup> in the tail of the beam.

The radial component of the equation of motion for electrons in the body of the beam is  $\ddot{r} - P_\theta^2/\gamma^2 m^2 r^3 = -\omega_\beta^2 r$ , where  $P_\theta$  is the canonical angular momentum, and the betatron frequency is

$$\omega_\beta^2 = 2(\beta c/r)^2 [i_b(r) - i_p(r)]/I_A$$

for a space-charge-neutralized beam. Here,  $i_b$  and  $i_p$  are the magnitudes of the beam and plasma currents inside the radius  $r$ . Whenever  $\omega_\beta^2 < P_\theta^2/\gamma^2 m^2 r^4$  the force on the beam electrons is repulsive. Current distributions monotonically decreasing in radius with induced plasma current exceeding the beam current inside of a particular radius produce a repulsive force on the beam electrons inside of that radius, triggering the hollowing.

The importance of avalanche ionization in the hollowing instability was established by Joyce and Lampe, who found that  $E/p$  must be greater than  $\sim 130 \text{ kV cm}^{-1} \text{ atm}^{-1}$  (in air) at its maximum near the pinch point for an  $n = 2$  instability to appear in the simulations.<sup>10</sup> The rate of generation of conductivity by the beam is

$$\partial\sigma/\partial t = c\kappa j_b + \nu_i\sigma - \alpha_r\sigma^2, \quad (1)$$

where the first term represents direct ionization by beam electrons and delta rays, the second, avalanche ionization, and the third, recombination. The avalanche-ionization rate,  $\nu_i$ , is a strong function of inductive electric field,  $E$ , and pressure,  $p$ , varying as  $(E/p)^n$ . In the parameter range of interest,  $n$  increases from  $n \sim 2$  (for  $E/p > 300 \text{ kV/cm} \cdot \text{atm}$ ) to  $n \sim 6$  (for  $E/p < 80 \text{ kV/cm} \cdot \text{atm}$ ). For a Bennett pinched beam with radius  $a$ , the electric field usually has the form

$$E_z \propto \ln \left( \frac{1 + b^2/a^2}{1 + r^2/a^2} \right), \quad (2)$$

which leads to an avalanche coefficient peaked on axis, because of its strong dependence on  $E$ . On-axis enhancement of conductivity can trigger the instability, because  $j_p = \sigma E$  is also peaked on axis. Because the nonlinearities of the equations greatly complicate analytical techniques, most studies have relied on particle-simulation methods, in which the complete self-consistent conductivity model of Eq. (1) can be included.

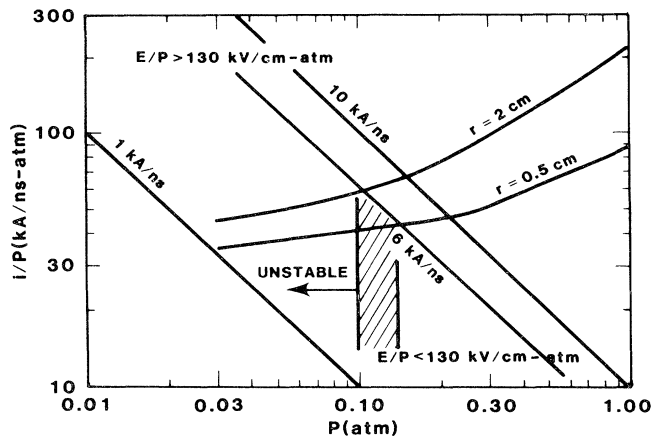


FIG. 1. Stability boundaries determined from CPROP simulations for beams with 0.5- and 2-cm radii. In the area above and to the left of the curves, the Joyce-Lampe criterion  $E/p = 130$  kV/cm·atm would be exceeded and the beam would be unstable (Ref. 10). On this graph, constant rates of current increase are plotted as straight lines. Thus, the 6-kA/ns IBEX beam is predicted to be unstable at pressures below the intersection of the 6-kA/ns line with the appropriate radius curve.

We performed experiments with the 4-MeV, 70-kA beam produced by the IBEX accelerator,<sup>14,15</sup> verifying the hollowing instability in air at pressures below the

predicted threshold. The rapid rise of beam current (4–6 kA/ns) allowed us to experiment in a regime where the threshold occurred at high pressures, where the air chemistry governing conductivity is reasonably well understood. Figure 1 depicts the 130-kV/cm-atm hollowing-instability threshold boundary for a range of air pressures, computed using CPROP.<sup>16</sup> The intersection of the current rise rate with the boundary predicts the beam to be unstable to hollowing at pressures of about 80 Torr and below.

CPROP is a version of the two-dimensional relativistic electromagnetic particle-in-cell beam simulation code CCUBE,<sup>17</sup> modified to include a moving coordinate mesh, an arbitrary conductivity field solver, and the BMCOND air chemistry package.<sup>18</sup> Peak electric fields near the beam head were determined from many short CPROP runs with various combinations of air pressure and beam current, rise time, and radius to obtain the data in Fig. 1. For economy, particles were held fixed in the beam frame. The peak electric field was found to depend only on current rise divided by pressure ( $\dot{i}/p$ ), pressure ( $p$ ), and beam radius ( $r$ ); the dependent on  $r$  is weak.

The IBEX diode produced a quiescent beam with a solid, Bennett-type profile with radius  $a \sim 0.7$  cm

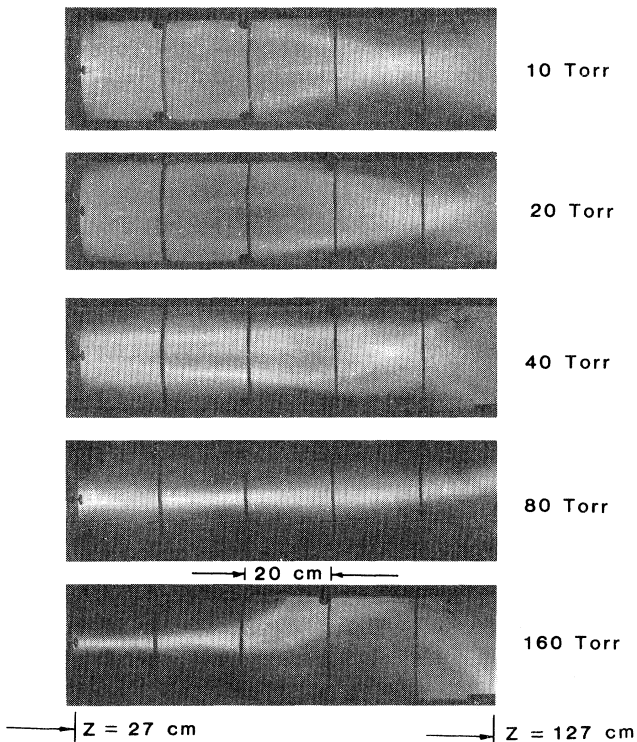


FIG. 2. Time-integrated photographs of beam-produced air fluorescence.

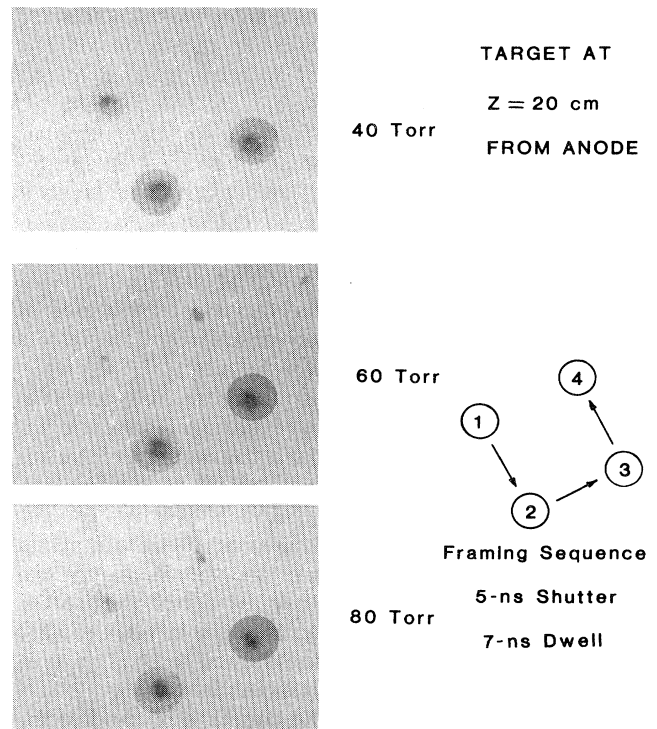


FIG. 3. Four-frame x-ray pinhole-camera images of the beam striking a 380- $\mu$ m-thick tantalum converter 20 cm from the anode. The small intense spot at the ten o'clock position in each circular frame is the image of the beam on the anode foil.

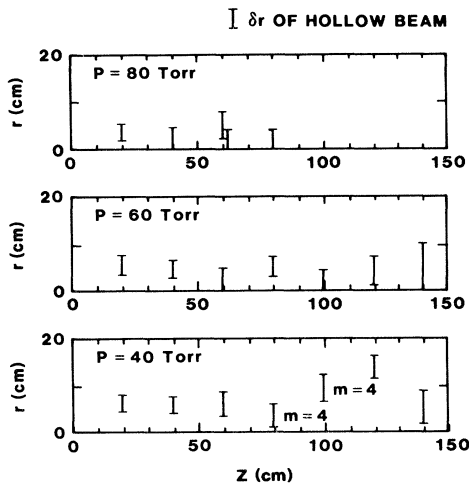


FIG. 4. Axial mode pattern determined from x-ray framing-camera data. Here,  $\delta r$  is the thickness of the hollow-beam annulus. Filamentation is noted by the dominant mode number observed.

measured with an x-ray framing camera.

The beam was injected into the 20-cm-radius propagation chamber through a 305- $\mu\text{m}$ -thick titanium anode that scattered the beam sufficiently to match it to the pinch force exerted by the  $\sim 20\text{-kA}$  net current. Increased foil scattering at early times in the pulse resulting from the voltage rise and scattering dependence on energy ( $\langle\theta\rangle \sim 1/\gamma$ ) also provided emittance tailoring of the beam head that may have helped to suppress the resistive hose.

We observed the hollowing instability of the beam as predicted. Time-integrated photographs of beam-excited air fluorescence clearly show the hose instability at high pressure, and hollowing at pressures below  $\sim 0.1$  atm (Fig. 2).

The most persuasive observations were time-resolved radiographs of the beam made with an x-ray framing camera. This four-frame pinhole camera used sealed microchannel-plate image intensifier tubes to image bremsstrahlung radiation from a thin tantalum

target foil, producing a 5-ns exposure each 7 ns. The target foil was tilted and viewed from an angle to displace the image of the anode from the image of the beam. These radiographs showed dramatic, large-amplitude hollowing at pressures of 60 Torr or less (Fig. 3), but only slight hollowing at 80 Torr.

The mode patterns obtained from radiographs of targets at different axial positions were strikingly similar to the mode patterns seen in computer simulations; compare Fig. 4 with Fig. 5, which shows instantaneous particle positions late into a laboratory-frame CPROP simulation of the IBEX beam in 40-Torr air. Simulations designed to model as closely as possible the actual experimental conditions were performed at 40, 80, 120, and 160 Torr. Large-amplitude, long-wavelength hollowing occurred in 40-Torr cases after the beam current reached its full value (Fig. 5). In contrast, 80-Torr simulations exhibited small-amplitude, short-wavelength hollowing. The 120-Torr runs, beyond the range of experimental pressures, only showed transitory hollowing early in the current rise. The beam was completely stable in 160-Torr simulations.

A dominant feature of the simulations was that the hollowing rapidly evolved into a standing wave in the laboratory frame, with the particles streaming through the stationary mode pattern shown in Fig. 5. This was also observed in the experiment; compare the beam radius in one frame of the x-ray data with that in the next frame, which is shuttered 7 ns later (Fig. 3). This is the reason that the hollowing is so pronounced in the time-integrated photographs (Fig. 2). The frozen-in nature of the instability results from the very long time needed for magnetic fields to decay in the high-conductivity plasma generated by the beam. The decay time was measured to be  $> 100$  ns at  $p \leq 80$  Torr, much longer than the  $\sim 20$ -ns beam duration.

We tested the conjecture that a peaked return-current profile is destabilizing by artificially spreading the return current with twelve axial copper wires equally spaced on a circle surrounding the beam. This stabilized the beam to the large-amplitude hollowing (Fig. 6).

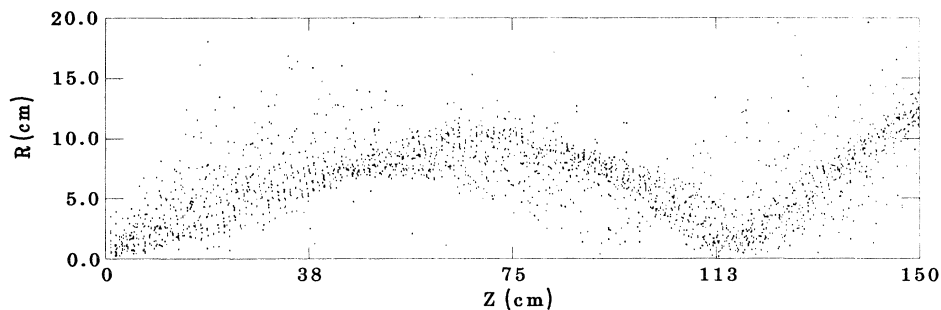


FIG. 5. Axial mode pattern from CPROP simulation. This is a standing wave in the laboratory frame, with the particles moving through the almost stationary pattern.

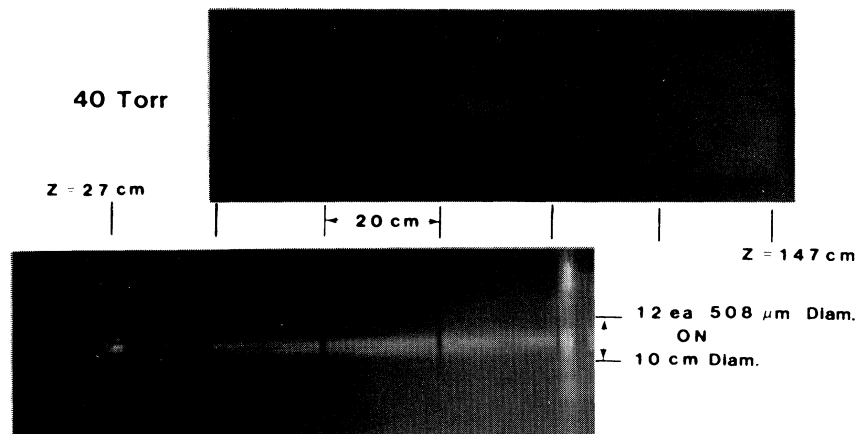


FIG. 6. Time-integrated photographs showing the stabilizing effect of surrounding the beam with twelve copper wires to artificially spread the conductivity.

The four-frame radiographs also revealed a tendency of the beam to tear into filaments after hollowing. The dominant mode numbers observed were  $3 < m < 6$ , although isolated instances of  $m$  as great as 10 were observed. Fully developed filamentation was observed only near or downstream from the node of the hollowing. The pressure threshold for filamentation must be lower than that for hollowing, because filamentation was never observed for  $p > 60$  Torr, while the hollowing threshold was somewhat in excess of 80 Torr.

In summary, we used the IBEX accelerator to produce a quiescent solid beam with a current rise time suitable for verifying theoretical predictions of the hollowing instability in an air pressure regime of interest. The beam became unstable in the pressure range predicted by simulations. Artificial spreading of the conductivity greatly reduced the instability amplitude, lending credence to the notion that a concentrated return current is necessary to trigger the instability. Finally, the beam tore into filaments after hollowing, an effect that could not have been predicted with the axisymmetric simulations.

This work was supported by the U. S. Department of Energy under Contract No. DE-AC04-DP00789, by the U. S. Air Force Weapons Laboratory, and by the Defense Advanced Research Projects Agency. The authors are indebted to R. Brown, D. Johnson, and L. Roose, who provided expert technical assistance in carrying out the experiments.

- <sup>1</sup>W. H. Bennett, *Phys. Rev.* **45**, 890 (1934).
- <sup>2</sup>W. H. Bennett, *Phys. Rev.* **98**, 1584 (1955).
- <sup>3</sup>M. N. Rosenbluth, *Phys. Fluids* **3**, 932 (1960).
- <sup>4</sup>S. Weinberg, *J. Math. Phys.* **8**, 614 (1967).
- <sup>5</sup>E. P. Lee, *Phys. Fluids* **21**, 1327 (1978).
- <sup>6</sup>F. W. Chambers, Lawrence Livermore National Laboratory Report No. UCID 18879, 1980 (unpublished).
- <sup>7</sup>E. P. Lee, Lawrence Livermore National Laboratory Report No. UCID 18940, 1981 (unpublished).
- <sup>8</sup>H. S. Uhm and M. Lampe, *Phys. Fluids* **25**, 1444 (1982).
- <sup>9</sup>H. C. Chen and H. S. Uhm, *Phys. Fluids* **26**, 3387 (1983).
- <sup>10</sup>G. Joyce and M. Lampe, *Phys. Fluids* **26**, 3377 (1983).
- <sup>11</sup>G. Benford, D. L. Book, and R. N. Sudan, *Phys. Fluids* **13**, 2621 (1970).
- <sup>12</sup>J. M. Leary and E. P. Lee, *Phys. Fluids* **15**, 716 (1972).
- <sup>13</sup>E. P. Lee and L. D. Pearlstein, *Phys. Fluids* **16**, 904 (1973).
- <sup>14</sup>R. B. Miller, M. G. Mazarakis, J. W. Poukey, and R. J. Adler, *IEEE Trans. Nucl. Sci.* **30**, 2722 (1983).
- <sup>15</sup>J. J. Ramirez, J. P. Corley, and M. G. Mazarakis, in *Proceedings of the Fifth International Conference on High Power Particle Beams*, San Francisco, 1983, edited by Richard J. Briggs and Alan J. Toepfer (Lawrence Livermore Laboratory, Livermore, California, 1983), p. 256.
- <sup>16</sup>B. B. Godfrey, *High Current Beam Propagation Study* (Mission Research Corp., Albuquerque, New Mexico, 1982), AMRC-R-367.
- <sup>17</sup>L. E. Thode, B. B. Godfrey, and W. R. Shanahan, *Phys. Fluids* **22**, 747 (1979).
- <sup>18</sup>R. L. Feinstein, unpublished.

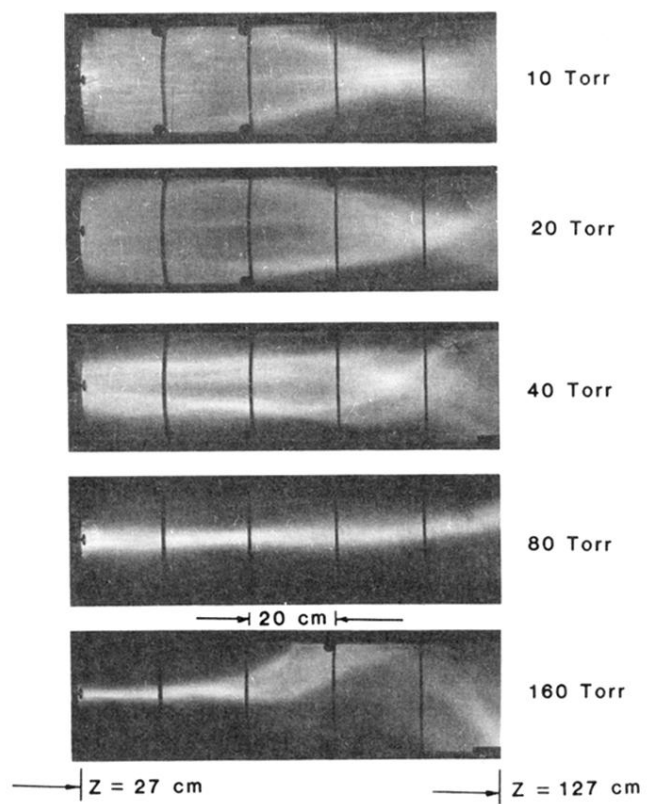


FIG. 2. Time-integrated photographs of beam-produced air fluorescence.

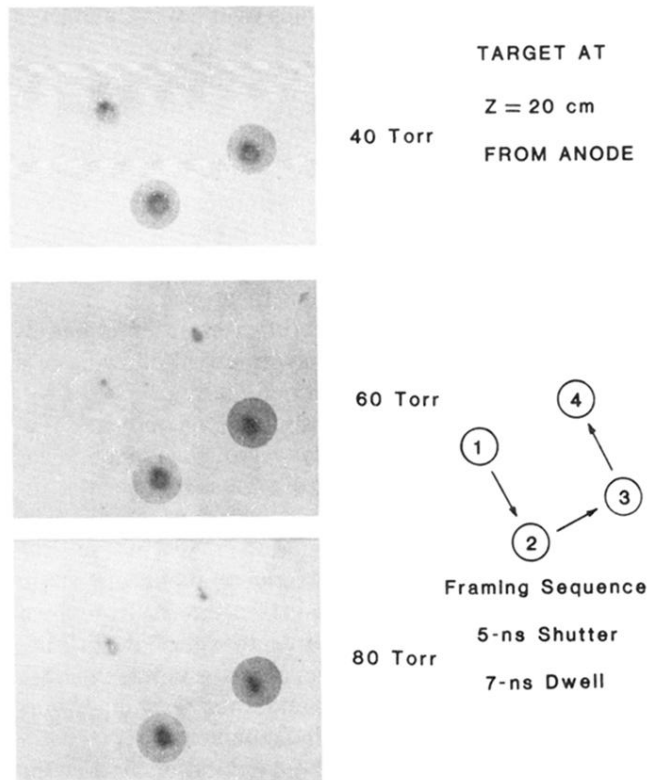


FIG. 3. Four-frame x-ray pinhole-camera images of the beam striking a 380- $\mu\text{m}$ -thick tantalum converter 20 cm from the anode. The small intense spot at the ten o'clock position in each circular frame is the image of the beam on the anode foil.

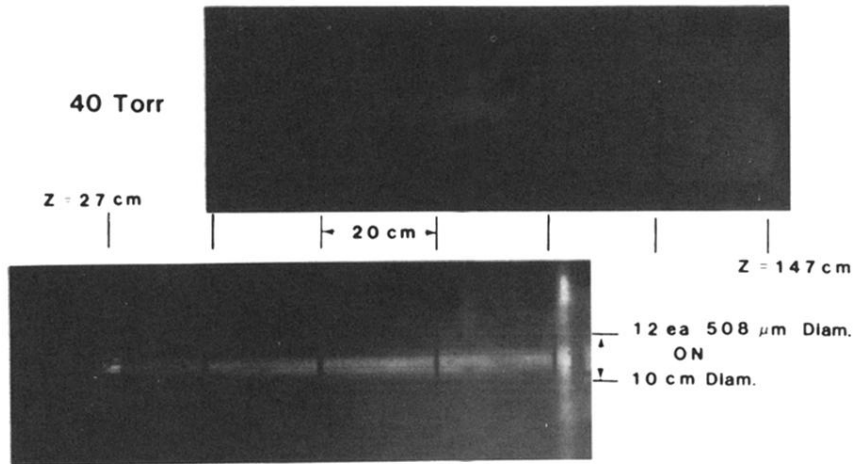


FIG. 6. Time-integrated photographs showing the stabilizing effect of surrounding the beam with twelve copper wires to artificially spread the conductivity.